ISSN : 0974 - 7486 Volume 7 Issue 1

Trade Science Inc.

Materials Science

An Indian Journal

Full Paper

MSAIJ, 7(1), 2011 [42-48]

Doped hydroxyapatite from waste calcium source: Part 1-Na doped apatite

Sumaya F.Kabir[2], Samina Ahmed[1]*, Mainul Ahsan[1], Ahmad I.Mustafa[2]

[1]Institute of Glass and Ceramic Research and Testing (IGCRT), Bangladesh Council of Scientific and Industrial Research (BCSIR), Dhaka-1205, (BANGLADESH)

[2]Department of Applied Chemistry and Chemical Engineering, University of Dhaka, Dhaka-1000, (BANGLADESH)

E-mail : bcsir@yahoo.com

Received: 16th August, 2010 ; Accepted: 26th August, 2010

ABSTRACT

Hydroxyapatite and its substituted forms are now finding potential applications as bone substitute materials. Particularly doped apatites with enhanced physical, chemical, mechanical and physiological stabilities have received significant attention. Following wet chemical precipitation approach Na doped hydroxyapatite bio-ceramic material has been successfully synthesized from egg shell for the first time. $(NH_4)_2HPO_4$ was used as the source of phosphate. Two different concentrations of doping solution were used to synthesize the doped apatite and the developed apatite was characterized by FTIR, XRF, XRD and SEM techniques. The analyses results were in excellent agreement with the standard values.

KEYWORDS

Na- doped apatite;
Bone substitute;
Biocompatible;
Calcium phosphate;
Calcination.

INTRODUCTION

Hydroxyapatite (HA), $Ca_{10}(PO4)_6(OH)_2$ a kind of bicompatible calcium phosphate bio-ceramic, has now received significant attention to the researchers as it mimics various properties of natural bone apatite[1-5]. This apatite due to its osteoconductivity has widely been used as a potential bioactive material for repairing bone or periodontal defects, bone replacement, augmentation of diseased bone or alveolar periodontal ridge, ear, eye implants, coating on femoral stems or acetabular cups, and bone substitution[1,2,6,7]. Vertebrate bone and tooth minerals contain HA with various substitution, such as Na^+, K^+, Mg^{2+}, Sr^{2+}, Cl^-, F^-, HPO_4^- etc.[8,9]. Substitution with different ions causes tremendous effects on physical, chemical, mechanical and physiological stabilities of HA[10]. Thus, considerable efforts have recently been conducted in developing substituted synthetic apatites involving the chemical species found in natural bone which could perform better bioactivity, osteoconductivity and biocompatibility[2,11].

Sodium is one of the important trace elements of human dental enamel and bone. This is an essential element in biological apatite for its potential role in cell adhesion, bone metabolism and resorption processes[12]. Moreover, Sodium acts as an essential nutrient with important functions in regulating extracellular fluid volume and the active transport of molecules across cell membrane[13]. A certain portion of this element is the prerequisite for better nerve and muscle functioning. To regulate fluids and blood pressure, and to keep muscles and nerves running smoothly, adults are required to take

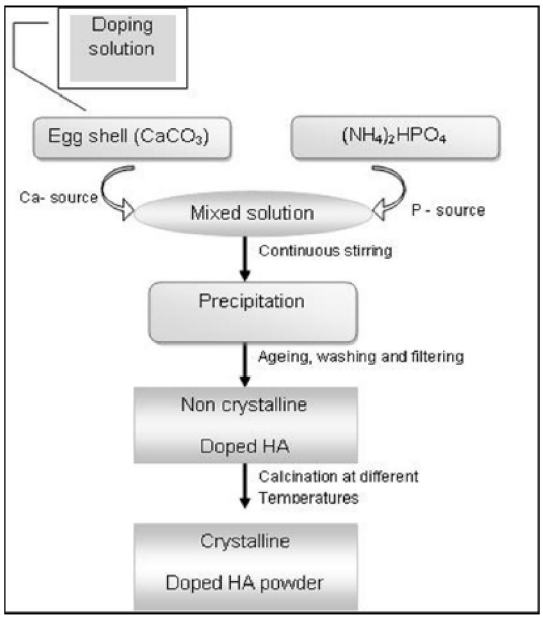

Figure 1 : Flow diagram of synthesis of doped HA

1,500 mg Na per day. In this regard, the sodium doped apatite would obviously act as a reservoir and carrier of sodium with better response in terms of the biological behavior and implantation. Considering the importance of doped hydroxyapatites, we have attempted to synthesize Na^{+}, Zn^{+2} and Fe^{+3} doped hydroxyapatite through a simple cost-effective procedure. Hence to the best of our knowledge for the first time we have synthesized doped hydroxyapatite using waste egg shell as the prime raw material of Ca-source. Egg shell is a waste material after the usage of egg and most of this waste is thrown away or disposed in landfills without any regard to the environment. In recent years, researchers have made their best efforts to utilize this "*waste to wealth*" and some notable applications of egg shell are: (i) synthesis of bone substitute, bio-ceramic materials[14,15-17]; (ii) low-cost adsorbent for waste water treatment[18,19]; (iii) low-cost solid catalyst for bio-diesel production[20] etc. Egg shell weighs ~11% of the total mass (ca. 60g) of egg and depending on feeding its chemical composition can be varied as follows: (94-97)% calcium carbonate and rest of the % contains magnesium carbonate, calcium phosphate and organic matter[16]. Utilization of egg shell to synthesize HA will benefit the mankind in two ways: firstly, this would able us to produce cost-effective bio-ceramic with better properties for therapeutic application and biological response and secondly, such raw material selection, would undoubtedly create an effective material-recycling pathway for waste management. However, in this paper we are describing only the synthesis and characterization of Na-doped HA.

EXPERIMENTAL

Materials

99.99% pure analar grade chemicals $NaNO_3$, NH_4OH, HNO_3, $(NH_4)_2HPO_4$ were obtained either from E. Merck or BDH and used in this study. All the solutions were prepared using double distilled water.

Synthesis of Na doped HA

Raw egg shells were first washed thoroughly with water and the inner membranes were removed. The shells were then boiled in aqueous medium for 30 minutes. After drying at 110°C all the egg shells were crushed to fine powder.

Sodium doped HA was synthesized by following a generalized wet chemical precipitation method. A requisite amount of egg shell powder was dissolved in conc. HNO_3 and 50 mL of distilled water was added to this acidic egg shell solution and filtered to get clear solution. Final volume was made up to 100 mL with distilled water maintaining the pH of the solution at ~10.0 with aqueous ammonia. The doping solution ($NaNO_3$) was mixed with the egg shell solution prior to the addition of phosphate precursor solution. $(NH_4)_2HPO_4$ in ammonia (pH~10.0) was added drop wise to this solution with continuous stirring condition. Yellowish gelatinous precipitates of doped HA was formed which was stirred for overnight in the mother solution for ripening. The precipitate was then filtered through a Buchner funnel and thoroughly washed with plenty of distilled water. At this stage, the filtered precipitate was dried at 110°C to remove any trace of water. The synthesized sample was then calcined at 900°C maintaining a fixed calcination time of 30 minutes. After calcination the sample was crushed to achieve fine powder. In order to investigate the concentration effect, $NaNO_3$ of 0.1M and 0.05 M was used in synthesis of Na doped HA and Ca/P molar ratio was maintained 1.66-1.69[14]. A pure stoichiometric HA (Ca/P=1.67) was also prepared following the above experimental procedure and was calcined at 900°C to compare the results. A flow

diagram of synthesis procedure is given in Figure 1.

Characterization

The egg shell powder was characterized through FTIR, XRD and SEM analysis which confirmed the presence of $CaCO_3$ and the percentage of $CaCO_3$ was determined by XRF.

Synthesized Na doped HA was first analyzed to examine the presence of Ca and P. Atomic absorption (AAS) and UV spectrophotometric methods were followed to detect these elements respectively. Fourier transform infrared spectroscopy (FT-IR, Model no. FT-IR 8900, SHIMADZU) was used to identify the functional groups. Experimental spectra were obtained by using KBr disks with a 1:100 "samples-to-KBr" ratio and the samples were scanned in the wave number range of 4000 cm^{-1}-400 cm^{-1} with an average of 30 scans. The resolution of the spectrometer was 4 cm^{-1}. Phase analysis of the prepared samples was performed by using PANalytical (X'Pert PRO XRD PW 3040). The intensity data were collected in 0.02° steps following the scanning range of 2θ=20°-80° using Cu$K\alpha$ (λ=1.54178°A) radiation. The observed phases were compared and confirmed using standard JCPDS files as described in the following section.

RESULTS

The recorded FTIR and XRD spectra of the egg shell powder are shown in figures 2 and 3 respectively while the morphology of the egg shells are shown in Figure 4 and 5 as observed by SEM.

Typical FTIR spectra of as received (oven dried at 110°C) and calcined (at 900°C) sodium substituted apatites, synthesized by using 0.1M doping solution are present in Figure 6 and 7. The XRD spectra captured in case of the 0.1 M Na-doped synthesized apatite (at 110°C and 900°C) are depicted in Figure 8 and 9 respectively. SEM micrograph of the calcined (at 900°C) doped apatites (synthesized by using 0.1 M and 0.05 M doping solution) are shown in Figure 10 and 11.

DISCUSSION

Characterization of egg shell

The amount of $CaCO_3$ present in the raw egg shell is ~ 95%, which is within the acceptable limit as found previously[21].

The FTIR spectrum (Figure 2) of egg shell powder showed the presence of same characteristic bands as those observed in natural calcite[22]. The observed bands at 1419 cm^{-1}, 873 cm^{-1}, 711 cm^{-1} were attributed to the asymmetric stretching and bending vibration mode of carbonate (CO_3^{2-}) group respectively[22]. A broad adsorption band around 3431.36 cm^{-1} was due to stretching vibration of structural water molecules[23] and the band situated at 2561.5 cm^{-1} is attributed to organic matter.

The diffraction patterns of the egg shell (Figure 3) are in excellent agreement with the JCPD files for rhombohedral calcite (File # 5-0586) as observed by Rivera et. al.[16]. The characteristic peak detected at 2θ position 29.485° (1 0 4) plane confirmed the mineral phase of egg shell as calcite and no other crystalline phase was observed. Using the Bragg reflections at (1 0 4) and (1 1 0) planes, the lattice parameters were measured as $a = b$ = 4.988°A and c =16.99°A, which are very close to those values calculated from JCPDS (File # 5-0586) reference data ($a = b$ = 4.983 °A and c =17.01°A).

The micro structural information of the inner part of the egg shell is visualized in Figure 4, which shows the presence of fibre-like morphology having similar pore size. On the other hand the magnified SEM picture (Figure 5) of the egg shell powder visualizes the interface between the smooth and granular regions where the aggregated smaller fractions are tied together by their organic components.

Characterization of Na doped HA

Chemical analysis

The preliminary characteristic analysis i.e. the presence of Na^+ ion in the substituted hydroxyapatites was confirmed by XRF analysis which also provided the Ca/P ratio as 1.67. This value matched with the Ca/P ratio of pure HA.

FTIR analysis

The observed characteristic peaks (Figure 6) representing the phosphate (PO_4^{3-}) group for the oven dried samples are appeared in broad fashion indicating poor crystalline and amorphous nature. Additionally peaks

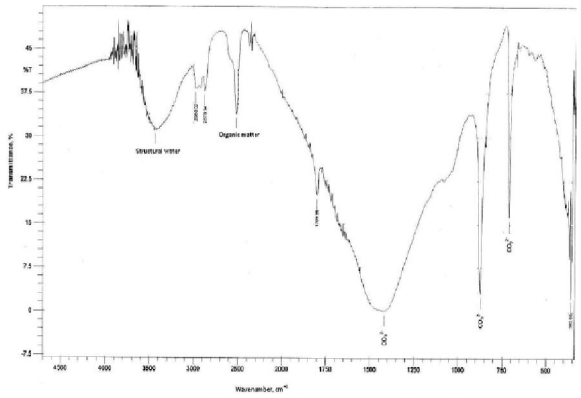

Figure 2 : FTIR spectrum of egg shell

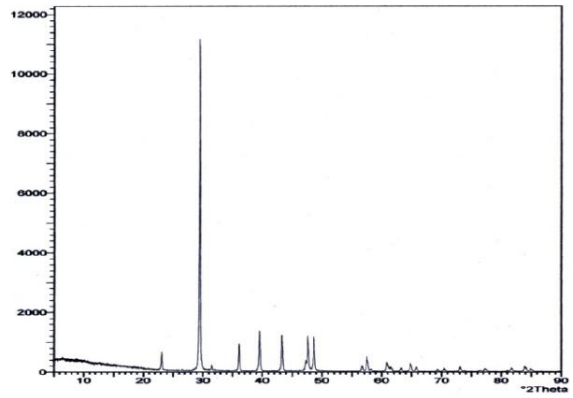

Figure 3 : XRD pattern for egg shell powder (dried at 110°C)

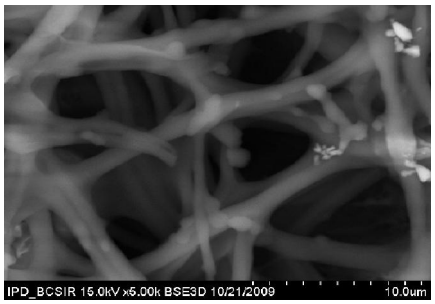

Figure 4 : SEM micrograph of inner part of egg shell

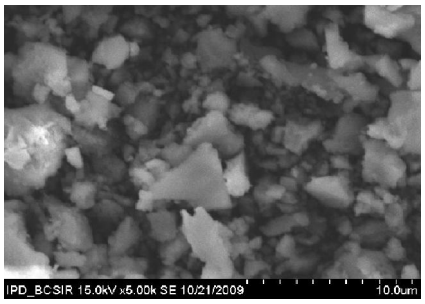

Figure 5 : SEM micrograph of egg shell powder

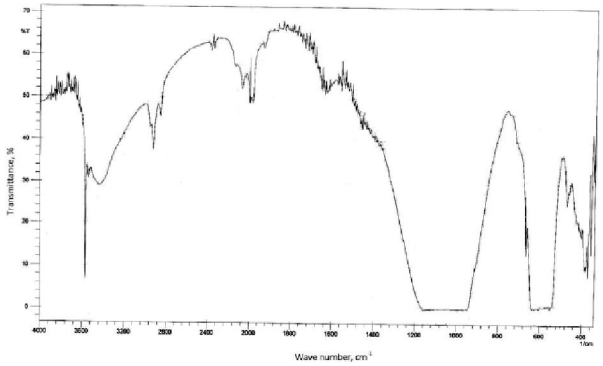

Figure 6 : FTIR spectrum of oven dried $Na_{(0.1M)}$ HA

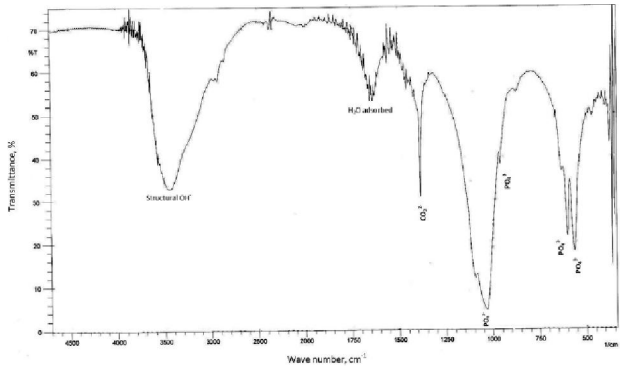

Figure 7 : FTIR spectrum of calcined $Na_{(0.1M)}$ HA

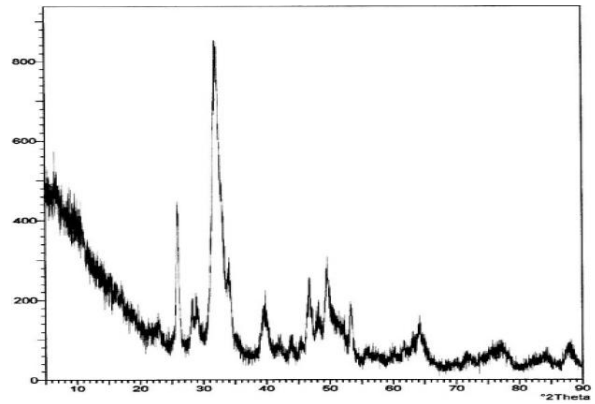

Figure 8 : XRD spectrum of oven dried $Na_{(0.1M)}$ HA

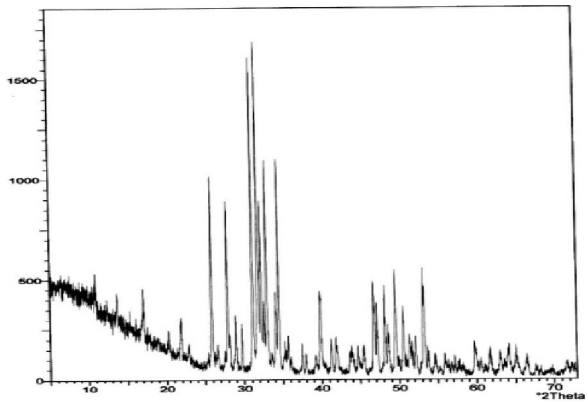

Figure 9 : XRD spectrum of calcined $Na_{(0.1M)}$ HA

Full Paper

TABLE 1 : FTIR band positions and corresponding assignments of calcined pure and Na cation doped apatites

Observed band positions (cm^{-1})			Corresponding assignments
Pure HA	$Na_{(0.05M)}$ HA	$Na_{(0.1M)}$ HA	
570.9	561.2	565.1	PO_4^{3-} bending (ν_4)
601.7	602.3	603.7	PO_4^{3-} bending (ν_4)
962.4	961.3	962.4	PO_4^{3-} stretching(ν_1)
1039.6	1016.2	1018.41	PO_4^{3-} bending (ν_3)
---------	1419.3	1423.47	CO_3^{2-} group (ν_3)
1650.0	1633.2	1639.4	H_2Oadsorbed(ν_2)
3500.00	3231.52	3431.3	Structural OH^-

for adsorbed water were also visible in this case. However, sintering (at 900°C) of this sample significantly transformed this amorphous nature to well crystalline form. The corresponding band positions representing the PO_4^{3-} group were evident as distinct, sharp peaks as expected (Figure 7). Particularly, the noticeable large separation between the band positions of PO_4^{3-} group at 565.1 and 603.7 cm^{-1} suggested the formation of crystallized apatitic phase[14]. This observation further satisfied by the XRD results as described in the following section. In figure 7 the presence of small peak for C-O vibration bonds of carbonate group at 1423 cm^{-1} suggested that this sample contained carbonate ion and the incorporation of cation is favored due to the presence of the carbonate ions[11]. The observed band positions and their respective assignments for 0.1 M and 0.05 M Na doped apatites are compared with the band positions of pure HA and summarized in TABLE 1. Clearly the good matching of the band positions showed that the synthesized Na-doped apatite resembles the nature of pure HA. This observation ensured the formation of the desired cation substituted HA within the present experimental protocol.

XRD analysis

The XRD spectrum (Figure 8) of the oven dried (at 110°C) doped apatite appeared with broad peaks showing the poorly crystalline phase together with amorphous phase supporting the observed FTIR data. This behaviour can be attributed to the temperature effect. It is well established that the increase in sintering temperature increases the crystallinity degree resulting several distinct peaks. This low crystallinity and amorphous nature have been dramatically changed to well-defined crystalline HA phase due to the thermal treatment[24] at

TABLE 2 : Relative intensity and *d*- spacing (hexagonal unit cell) for calcined pure HA and Na doped HA

$Na_{(0.1)}$ HA		$Na_{(0.05)}$ HA		Pure HA	
d-spacing	relative intensity	*d*-spacing	relative intensity	*d*-spacing	relative intensity
4.0786	15.94	4.0790	11.32	4.0748	6.38
3.8751	15.42	3.888	7.31	3.8999	4.45
3.4384	62.06	3.4362	57.16	3.4395	38.68
3.1692	11.25	3.1659	11.57	3.1673	8.36
3.0776	15.70	3.0794	18.76	3.0861	14.60
2.8117	100.00	2.8097	100.00	2.8152	100.00
2.7750	50.64	2.7735	53.18	2.7744	59.40
2.7161	66.92	2.7153	61.50	2.7183	55.42
2.6280	24.93	2.6267	25.97	2.6296	23.44
2.5135	12.20	2.5108	7.98	2.5271	5.30
2.2614	26.13	2.2616	23.74	2.2619	19.31
2.1461	8.83	2.1474	7.97	2.1482	5.28
2.0617	29.03	2.0605	24.43	2.0610	5.54
1.9423	25.30	1.9431	14.44	1.9443	28.19
1.8888	32.90	1.8893	33.77	1.8914	14.58
1.8395	20.40	1.8400	17.52	1.8413	32.19
1.8054	12.39	1.8039	11.51	1.8060	15.67
1.7792	11.04	1.7780	13.37	1.7806	11.83
1.7538	27.85	1.752	11.94	1.7538	12.30

900°C (Figure 9). The observed intensity and d-spacing values are in excellent agreement with the JCPDS standard data (ref. code: 09-0432) for HA as shown in TABLE 2. Particularly the strong diffraction peaks matched with the characteristics peaks for pure HA (at 900°C) at 2θ positions ~31.78° (2 1 1) together with other two peaks at ~32.26° (1 1 2) and ~32.95° (3 0 0) having similar intensities. This observation ensured the formation of Na substituted apatite of hexagonal structure and strictly proved that the HA structure welcomes a variety of substitutions of both cationic and anionic without any significant modification in its hexagonal system as mentioned in the previous investigation[11].

The crystallite size of Na doped (0.1 M and 0.05 M) calcined (at 900°C) apatites was calculated using Scherrer's relationship,

$$D = 79.5/\Delta \cos\theta \quad (1)$$

where, D = crystal size, Δ= FWHM in degree. The Bragg reflections at (211), (112) and (300) planes were considered to calculate the crystallite size while the crystallinity and cell volume were calculated from the following equations 2 and 3 respectively. The values are

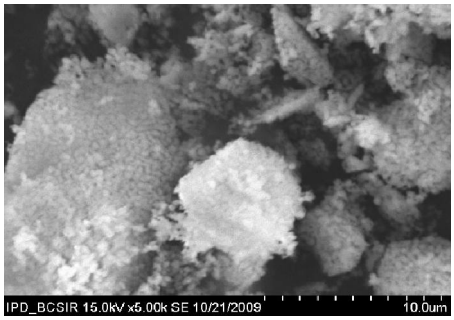

Figure 10 : SEM micrograph of $Na_{(0.1M)}HA$ at 900°C

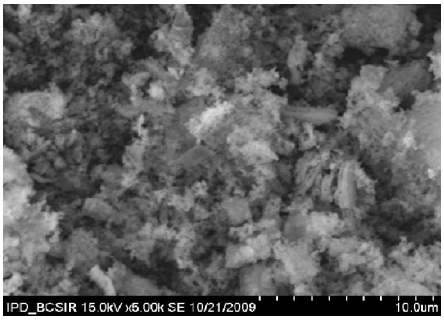

Figure 11 : SEM micrograph of $Na_{(0.05M)}$ HA at 900°C

TABLE 3 : Crystallographic information of clacined pure and substituted apatites

Parameters	Calcined $Na_{(0.05M)}HA$	Calcined $Na_{(0.1M)}HA$	Calcined HA
Lattice parameter *a=b*	9.39	9.38	9.42
c	6.85	6.85	6.88
Crystallinity, x_c	3.54	3.54	5.03
Crystal size (°A)	471.35	505.81	752.37
Volume	1563.70	1560.02	1580.60

summarized in TABLE 3.

$$\text{Crystallinity, } X_c = \left(\frac{k_a}{\Delta}\right)^3 \quad (2)$$

where, Δ=FWHM of the (002) reflection and $k_a = 0.24$

Cell volume $V=2.589a^2c$ (3)

Clearly, the lattice parameters, crystallite size, crystallinity and cell volume of the Na-doped apatites were lower than that of pure HA, as substitution reduces significantly the crystallite size as well as crystallinity[7]. Changes in cell volume could be explained due to the effect of smaller cation size of Na than that of Ca. Incorporated of this smaller cation into the apatite structure resulted in shrinkage of volume[3].

SEM analysis

Since the formation of crystalline apatites strictly depends on the sintering temperature and as a consequence it has already been evident that synthesized apatite is produced in well crystalline form only after sintering at 900°C, so the morphology and micro structural features of the crystalline Na substituted apatites formed at this temperature were further investigated by capturing their SEM micrographs. The recorded SEM pictures (Figure 10 and 11) for calcined (at 900°C) apatites visualized a combination of different regular shapes, such as hexagonal, spherical, etc. which were agglomerated.

CONCLUSION

Using the egg shell as the prime source of Ca, sodium (Na) substituted or doped hydroxyapatite has been synthesized, which could be a potential and cost-effective bio-ceramic material for bone substitution in surgery, orthopedics and dentistry fields. The synthesized doped apatites were characterized by XRF, FTIR, XRD and SEM techniques. The change in concentration of doping solution did not affect the formation of desired doped apatite. However, incorporation of such cation in hydroxyapatite structure is supposed to improve the bioactivity and physiochemical properties of the apatite. On the other hand utilization of egg shell will be an effective pathway for waste management through material re-cycling approach.

ACKNOWLEDGEMENT

The authors gratefully acknowledge the financial support from IGCRT, BCSIR and the assistance of Dr. Mohammad Mizanur Rahman, Assistant Professor of ACCE, DU for FTIR. Thank is also due to the Ministry of Science and Information & Communication Technology, Government of Bangladesh for granting NSICT fellowship to SFK.

REFERENCES

[1] S.J.Kalita, H.A.Bhatt; Materials Science and Engineering C, **27**, 837-848 **(2007)**.
[2] F.Ren, R.Xin, X.Ge, Y.Leng; Acta Biomaterialia, **5(8),** 3141-3149 **(2009)**.
[3] T.J.Webster, E.A.Massa-Schlueter, J.L.Smith, E.B.Slamovich; Biomaterials, **25**, 2111-2133 **(2004)**.

[4] M.E.Fleet, Xi Liu; Biomaterials, **28**, 916-926 **(2007)**.

[5] F.Miyaji, Y.Kono , Y.Suyama**;** Materials Research Bulletin, **40**, 209-220 **(2005)**.

[6] D.K.Pattanayak, R.Dash, R.C.Prasad, B.T.Rao, T.R.Mohan; Materials Science and Engineering C, 684-690 **(2007)**.

[7] H.S.Azevedo, I.B.Leonor, C.M.Alves, R.L.Reis; Materials Science and Engineering C, **25**, 169-179 **(2005)**.

[8] I.R.de Lima, A.M.Costa, I.N.Bastos, J.M.Granejeiro, G.de Almeida Soares; Materials Research, **9**, 399-403 **(2006)**.

[9] M.'O Li, X.Xiao, R.Liu, C.Chen, L.Huang; J.Mater.Sci.Mater.Med, **19**, 797-803 **(2008)**.

[10] Y.Tang, H.F.Chappell, M.T.Dove, R.J.Reeder, Y.J.Lee; Biomaterials, **30**, 2864-2872 **(2009)**.

[11] S.Kannan, F.Goetz-Neunhoeffer, J.Neubauer, J.M.F.Ferreira; J.Am.Ceram.Soc., **91(1)**, 1-12 **(2008)**.

[12] S.Kannan, J.M.G.Ventura, A.F.Lemos, A.Barba, J.M.F.Ferreira; Ceramics International, **34**, 7-13 **(2008)**.

[13] M.E.Doyle, K.A.Glass; Food Science and Technology, **9**, 44-56 **(2009)**.

[14] S.Ahmed, M.Ahsan; Bangladesh J.Sci.Ind.Res., **43(4)**, 501-512 **(2008)**.

[15] C.Balazsi, F.Weber, Z.Kover, E.Horváth, C.Németh; J.Euro.Ceram.Soc.**, 27**, 1601 **(2007)**.

[16] E.M.Rivera, M.Araiza, W.Brostow, V.M.Castaño, J.R.Díaz-Estrada, R.Hernández, J.R.Rudriguez; Mat.Lett., **41**, 128 **(1999)**.

[17] K.Prabakaran, A.Balamurugan, S.Rajeswari; Bull.Mater.Sci., **28**, 115 **(2005)**.

[18] K.Chojnacka, J.Hazardous; Mat.B, **121**, 167 **(2005)**.

[19] W.T.Tsai, K.J.Hsien, H.C.Hsu, C.M.Lin, K.Y.Lin, C.H.Chiu; Biores.Technol., **99**, 1623 **(2008)**.

[20] Z.Wei, C.Xu, B.Li; Biores.Technol., **100**, 2883 **(2009)**.

[21] K.Prabakaran, A.Balamurugan, S.Rajeswari; Mater.Sci., **28(2)** 115 **(2005)**.

[22] R.Z.Le Geros, J.P.Le Geros, O.R.Trautz, E.Klein; Plenum Press, New York, 3-12 **(1970)**.

[23] V.Michel, Ph.IIdefonse, G.Morin; Palaeoecol, **126**, 109-119 **(1996)**.

[24] W.Feng, L.Mu-Sen, L.Yu-Peng, Q.Yong-Xin; Mater.Lett, **59**, 916 **(2005)**.